2nd-Order CESE Results For C1.4: Vortex Transport by Uniform Flow

David J. Friedlander

NASA Glenn Research Center, Cleveland, OH, 44135

1 Code Description

The Conservation Element and Solution Element (CESE) method [1, 2] was used as implemented in the NASA research code ez4d [3]. The CESE method is a time accurate formulation with flux-conservation in both space and time. The method treats the discretized derivatives of space and time identically and utilizes a staggered mesh approach consisting of conservation elements (CE) and solution elements (SE). While high-order versions of the method exist [4, 5, 6], the 2nd-order accurate version was used. In regards to the ez4d code, it is an unstructured Navier-Stokes solver coded in C++ with serial and parallel versions available. As part of its architecture, ez4d has the capability to utilize multi-thread and Messaging Passage Interface (MPI) for parallel runs.

2 Meshes

Three sets of meshes were used for the computations: the 2D and randomly perturbed (RP) meshes provided by the workshop and a set of meshes made from scratch using Pointwise®. The meshes made from scratch were formed by producing a uniformly spaced structured grid and then diagonalizing it by dividing each cell into two triangular cells using the "best fit" option within Pointwise®. The 2D and RP meshes were run on grid levels 3 and 4 while the diagonalized structured (DS) meshes were run on grid levels 3 through 5. Domain sizes for the various meshes are shown in Table 1. For the boundary conditions (bc), periodic boundary conditions were applied to the left and right boundaries of the domains while a non-reflecting boundary condition was applied to the top and bottom boundaries of the domains. Additional cases using the DS meshes were run with periodic boundary conditions for all boundaries of the domains.

Table 1: Domain Sizes

Grid Level	i Dimension	j Dimension	2D Cells	RP Cells	DS Cells
3	128	128	32,768	32,768	32,768
4	256	256	131,072	131,072	131,072
5	512	512	-	-	524,288

3 Case Summary

A summary of case configurations is shown in Table 2. Cases utilizing a single core were run on an Intel Xeon W3680 core with times for running the TauBench executable ranging from 7.998s to 8.415s with an average of 8.141s. Cases utilizing multiple cores were run on Intel Xeon X5670 cores (NASA Pleiades, Westmere) with times for running the TauBench executable ranging from 8.689s to 8.741s with an average of 8.717s. All cases were run out to an equivalent time of 50 time periods.

Table 2: Case Configurations

Case #	# of Cores	Mesh Type	Grid Levels	Top/Bottom BC	Vortex Speed
1	1	2D	3-4	Non-Reflecting	Fast
2	1	RP	3-4	Non-Reflecting	Fast
3	1	DS	3-4	Non-Reflecting	Fast
4	12	DS	5	Non-Reflecting	Fast
5	12	DS	3-5	Periodic	Fast
6	48	DS	3-5	Periodic	Slow

4 Results

4.1 Fast Vortex Cases

Non-dimensional u velocity contours for the fast vortex cases are shown in Fig. 1 through Fig. 4. Note that the velocity contours are non-dimensionalized by the freestream u velocity. It can seen that the vortex core strength decreases over time and that the vortex as a whole drifts down and to the right. Trends are similar for all grid and boundary condition sets and mesh refinement shows improvement in minimizing both the vortex core strength decay and the vortex drifting.

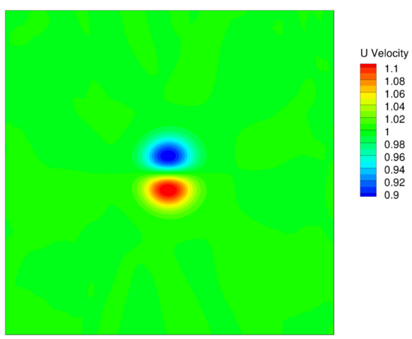

(a) Level 3, T=1

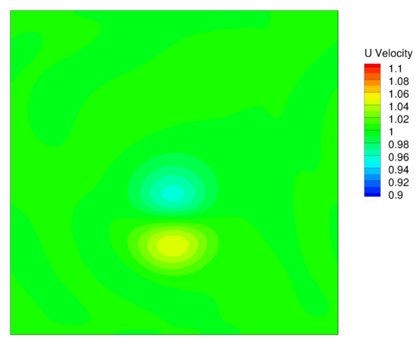

(b) Level 3, T=50

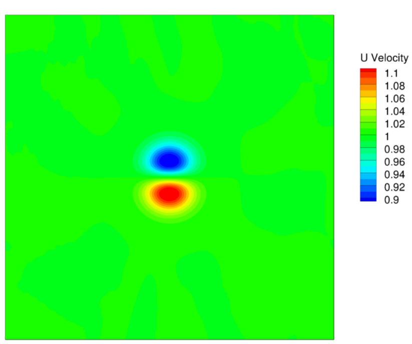

(c) Level 4, T=1

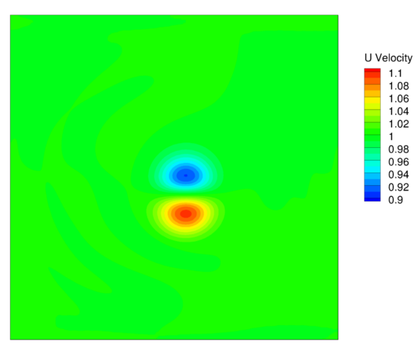

(d) Level 4, T=50

Figure 1: Non-dimensional u velocity contours for the fast vortex on the 2D grids (with non-reflecting bc).

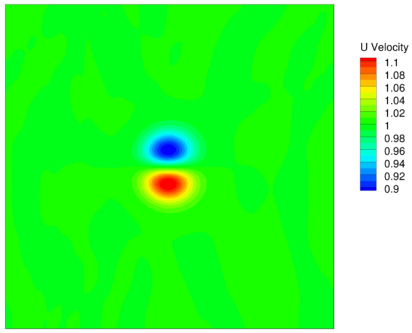

(a) Level 3, T=1

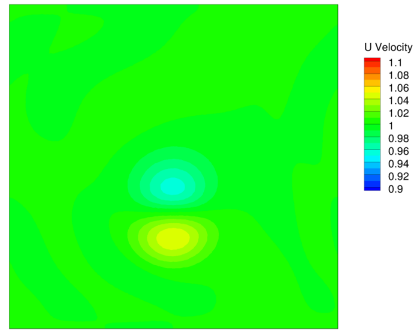

(b) Level 3, T=50

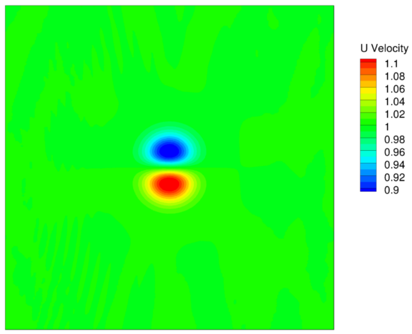

(c) Level 4, T=1

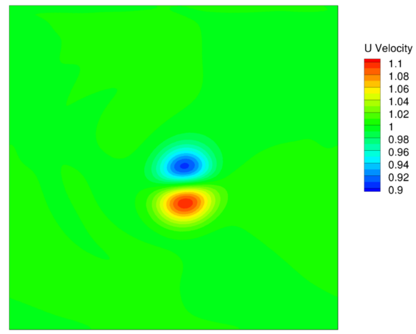

(d) Level 4, T=50

Figure 2: Non-dimensional u velocity contours for the fast vortex on the RP grids (with non-reflecting bc).

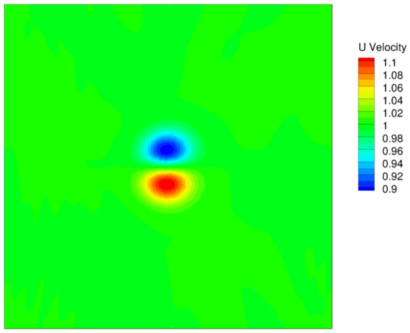

(a) Level 3, T=1

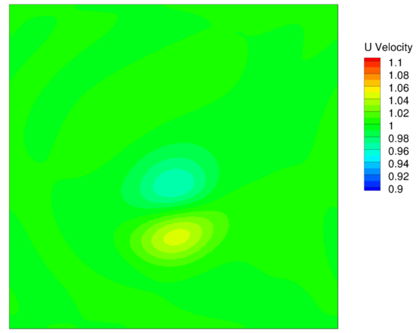

(b) Level 3, T=50

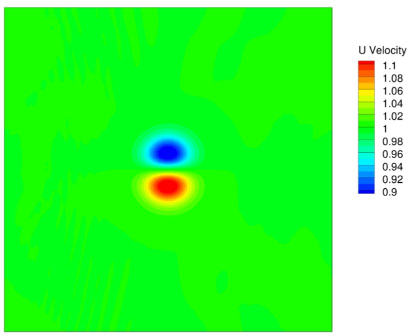

(c) Level 4, T=1

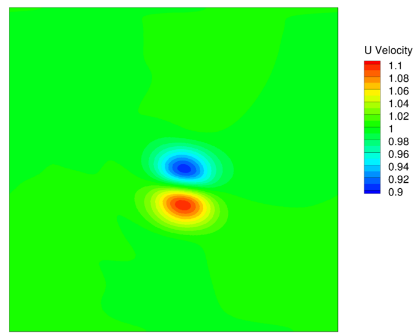

(d) Level 4, T=50

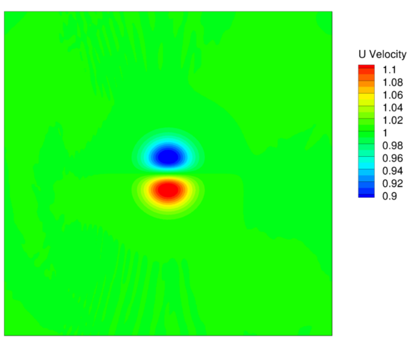

(e) Level 5, T=1

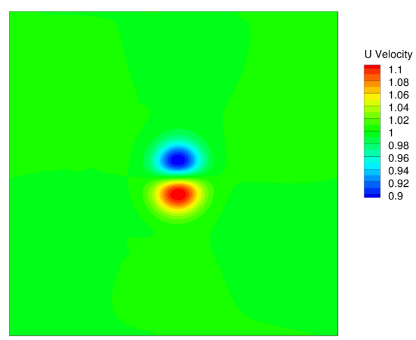

(f) Level 5, T=50

Figure 3: Non-dimensional u velocity contours for the fast vortex on the DS grids (with non-reflecting bc).

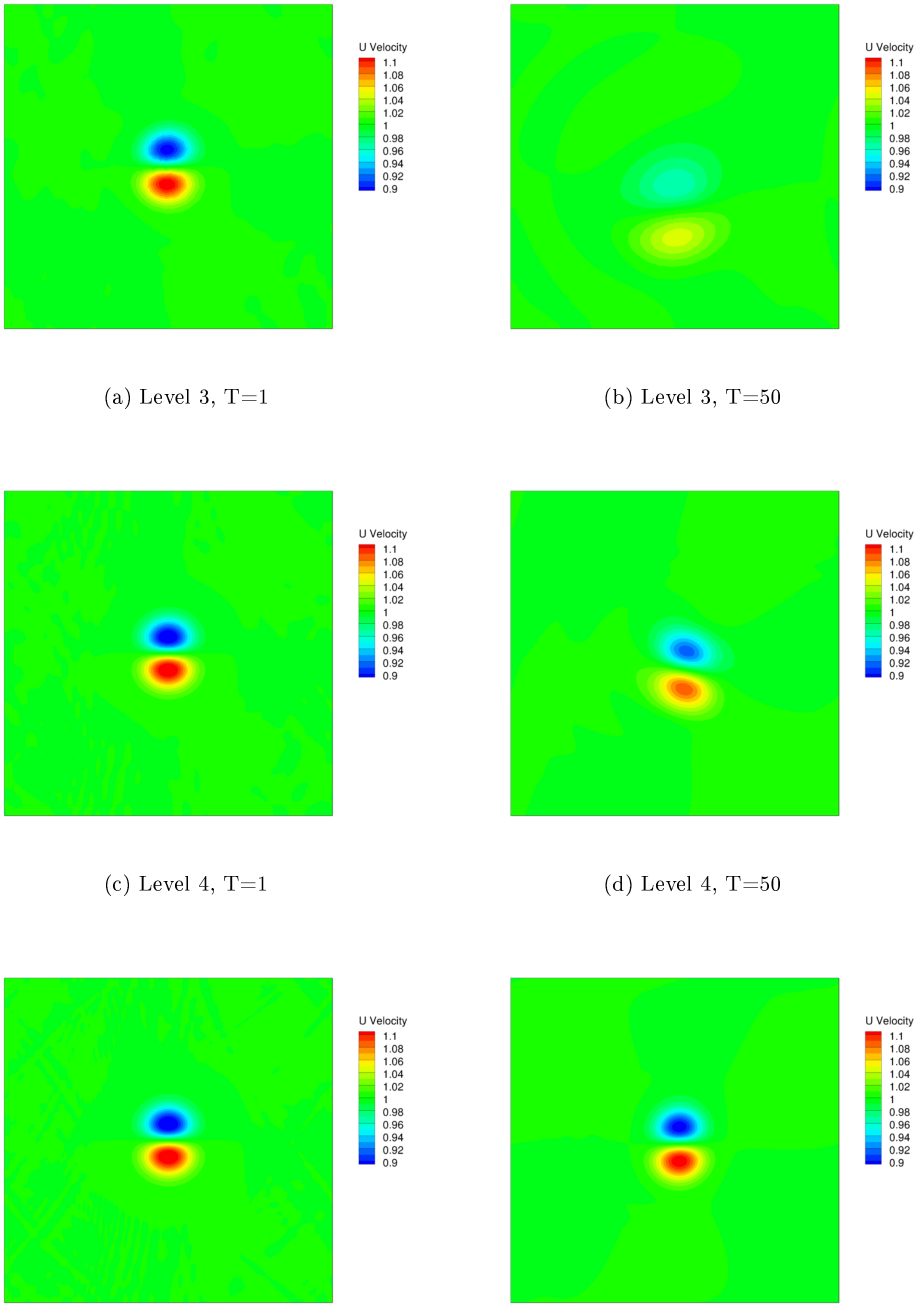

(a) Level 3, T=1

(b) Level 3, T=50

(c) Level 4, T=1

(d) Level 4, T=50

(e) Level 5, T=1

(f) Level 5, T=50

Figure 4: Non-dimensional u velocity contours for the fast vortex on the DS grids (all periodic bc).

The workshop requires the L2 norm of the u and v velocity errors of the 50 time period solution to be computed and compared to the work units and length scale for each grid. The u and v velocity L2 norms were computed as follows:

$$Error_{L2(u)} = \sqrt{\frac{\sum_{i=1}^{N} \int_{V_i} (u_i - u_{initial,i})^2 \, dV}{\sum_{i=1}^{N} |V_i|}} \tag{1}$$

$$Error_{L2(v)} = \sqrt{\frac{\sum_{i=1}^{N} \int_{V_i} (v_i - v_{initial,i})^2 \, dV}{\sum_{i=1}^{N} |V_i|}} \tag{2}$$

The work units were defined as the time it took ez4d to run the entire simulation normalized by the time it took to run the TauBench executable.

$$WorkUnit = \frac{t_{ez4d}}{t_{TauBench}} \tag{3}$$

In addition, the length scale was defined as:

$$h = \frac{1}{\sqrt{nDOF}} = \frac{1}{\sqrt{n_{cells}}} \tag{4}$$

Figure 5 shows the u velocity errors verses work units and length scale while Fig. 6 shows the v velocity errors verses work units and length scale. It can be seen that the velocity errors are mostly independent of the grid configuration (i.e. 2D, RP, DS) and only dependent on the number of grid cells. Also, it can be seen that the velocity errors are nearly independent of the boundary condition applied to the top and bottom of the domains. As expected, the u and v velocity errors decrease with decreasing length scale (and subsequently with increasing work units).

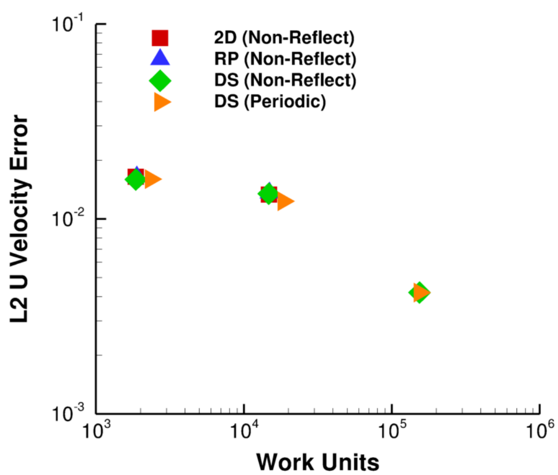

(a) Error verses work units.

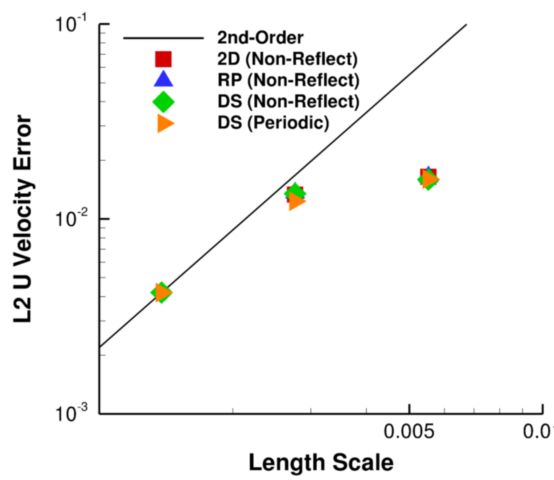

(b) Error verses length scale.

Figure 5: Workshop metric results for the u velocity error, fast vortex.

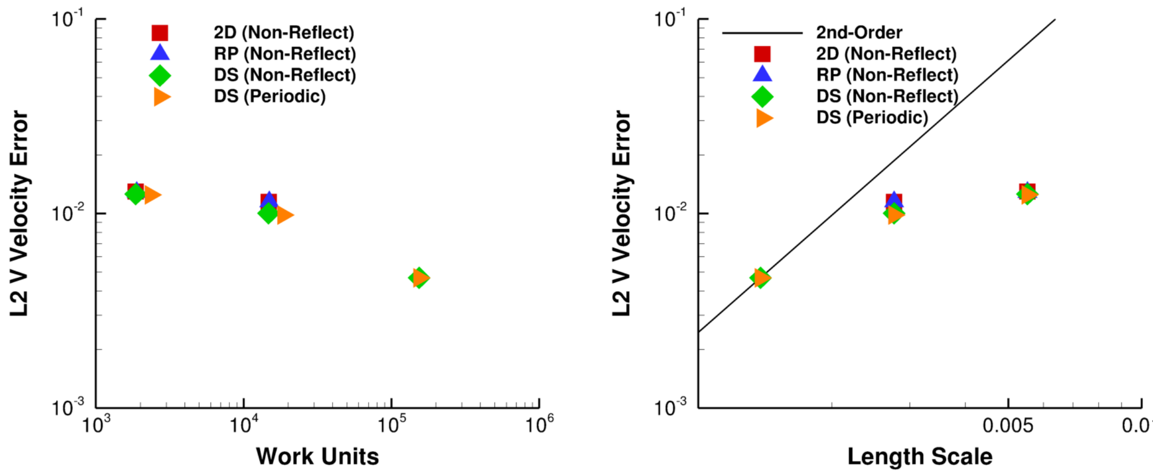

(a) Error verses work units.

(b) Error verses length scale.

Figure 6: Workshop metric results for the v velocity error, fast vortex.

4.2 Slow Vortex Cases

Because the fast vortex cases showed little sensitivity to mesh type and to the top/bottom boundary conditions, the slow vortex cases were run only on the DS meshes with all periodic boundary conditions. Figure 7 shows the L2 velocity errors verses work units and length scale for the slow vortex cases. As expected, the u and v velocity errors decrease with decreasing length scale (and subsequently with increasing work units). In addition, non-dimensional u velocity contours are shown in Fig. 8. Like the previous fast vortex contours, the velocity contours are non-dimensionalized by the freestream u velocity. Trends are similar to that of the fast vortex cases and mesh refinement shows improvement in minimizing the vortex core strength decay.

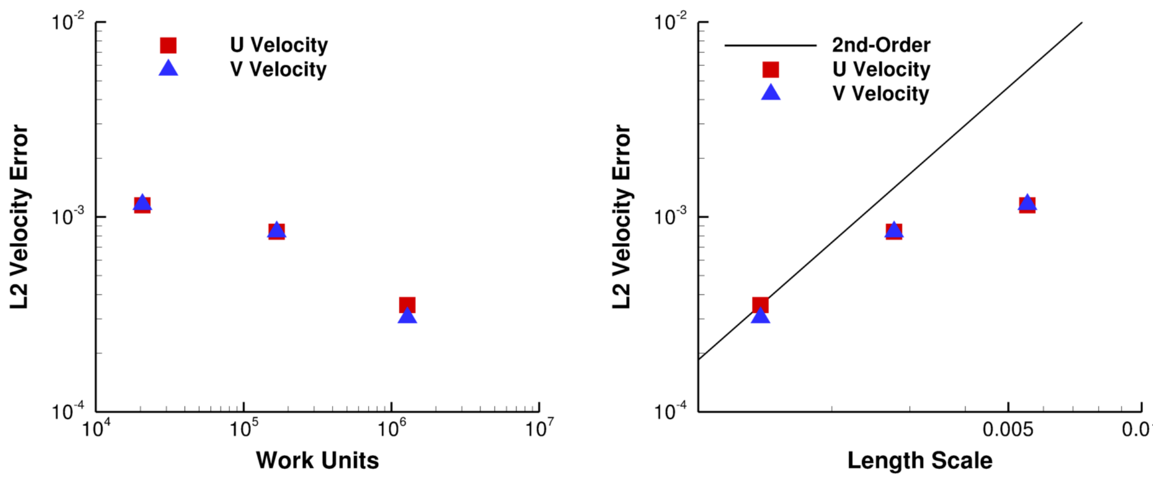

(a) Error verses work units.

(b) Error verses length scale.

Figure 7: Workshop metric results for the slow vortex cases.

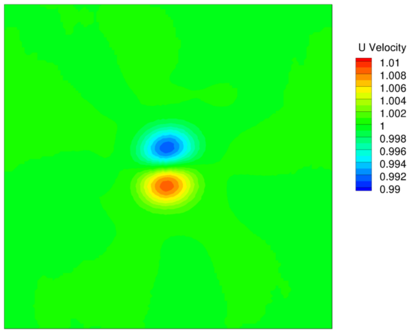

(a) Level 3, T=1

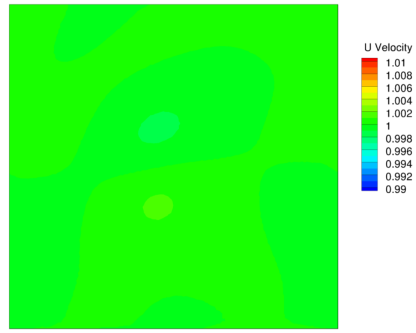

(b) Level 3, T=50

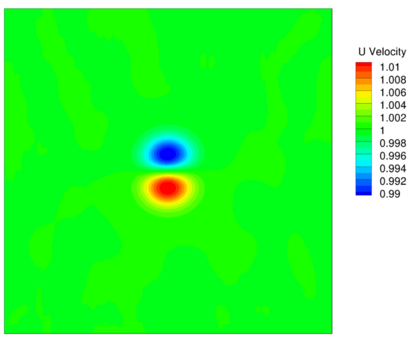

(c) Level 4, T=1

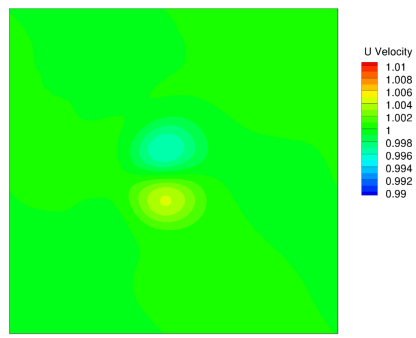

(d) Level 4, T=50

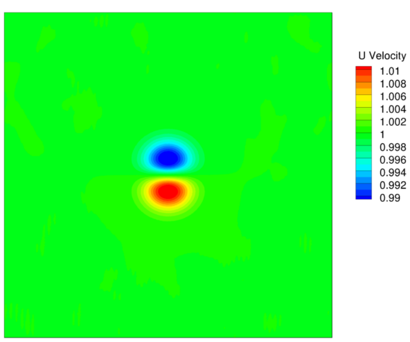

(e) Level 5, T=1

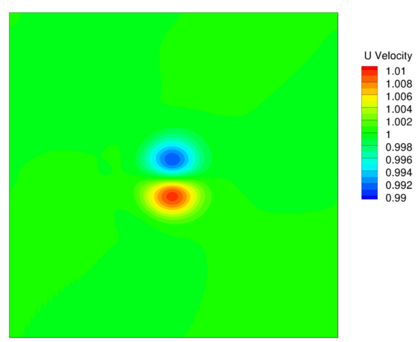

(f) Level 5, T=50

Figure 8: Non-dimensional u velocity contours for the slow vortex on the DS grids (all periodic bc).

Acknowledgments

The author would like to thank the Aerosciences Project under the NASA Fundamental Aeronautics Program for support with this effort as well as Chau-Lynn Chang and Balaji Venkatachari for guidance and support with using the ez4d code.

References

[1] Chang, S. C., "The Method of Space-Time Conservation Element and Solution Element - A New Approach for Solving the Navier-Stokes and Euler Equations," *Journal of Computational Physics*, Vol. 119, No. 2, 1995, pp. 295–325.

[2] Chang, S. C., Wang, X. Y., and Chow, C. Y., "The Space-Time Conservation Element and Solution Element Method - A New Resolution and Genuinely Multidimensional Paradigm for Solving Conservation Laws," *Journal of Computational Physics*, Vol. 156, No. 1, 1999, pp. 89–136.

[3] Chang, C. L., "Time-Accurate, Unstructured-Mesh Navier-Stokes Computations with the Space-Time CESE Method," Tech. Rep. AIAA 2006-4780, July 2006.

[4] Venkatachari, B., Cheng, G., and Chang, S. C., "Development of a High-Order CESE Scheme For Transient Viscous Flows," Tech. Rep. AIAA 2009-3984, June 2009.

[5] Chang, S. C., "A New Approach for Constructing Highly Stable High Order CESE Schemes," Tech. Rep. AIAA 2010-543, January 2010.

[6] Chang, C. L., Venkatachari, B., and Cheng, G., "Time-Accurate Local Time Stepping and High-Order Space-Time CESE Methods for Multi-Dimensional Flows with Unstructured Meshes," Tech. Rep. AIAA 2013-3069, June 2013.